1-GHz repetition rate femtosecond OPO with stabilized offset between signal and idler frequency combs

R. Gebs[1], T. Dekorsy[1], S. A. Diddams[2], A. Bartels[1]

[1]*Center for Applied Photonics, University of Konstanz, Universitätsstrasse 10, 78457 Konstanz, Germany*
[2]*National Institute of Standards and Technology, 325 Broadway, Mail Stop 847, Boulder, Colorado 80305, USA*
Raphael.Gebs@uni-konstanz.de

Abstract: We report an optical parametric oscillator (OPO) based on periodically poled lithium niobate (PPLN) that is synchronously pumped by a femtosecond Ti:sapphire laser at 1 GHz repetition rate. The signal output has a center wavelength of 1558 nm and its spectral bandwidth amounts to 40 nm. The OPO operates in a regime where the signal- and idler frequency combs exhibit a partial overlap around 1600 nm. In this near-degeneracy region, a beat at the offset between the signal and idler frequency combs is detected. Phase-locking this beat to an external reference stabilizes the spectral envelopes of the signal- and idler output. At the same time, the underlying frequency combs are stabilized relative to each other with an instability of 1.5×10^{-17} at 1 s gate time.

References and links

1. S. A. Diddams, J. C. Bergquist, S. R. Jefferts, C.W. Oates, "Standards of time and frequency at the outset of the 21st century," Science **306**, 1318-1324 (2004).
2. S. A. Diddams, Th. Udem, J. C. Bergquist, E. A. Curtis, R. E. Drullinger, L. Hollberg, W. M. Itano, W. D. Lee, C. W. Oates, K. R. Vogel, D. J. Wineland, "An optical clock based on a single trapped ^{199}Hg$^+$ ion," Science **293**, 825-828 (2001).
3. M. Takamoto, F. L. Hong, R. Higashi, H. Katori, "An optical lattice clock," Nature (London) **435**, 321-324 (2005).
4. H. G. Dehmelt, "Mono-ion oscillator as potential ultimate laser frequency standard," IEEE Trans. Instrum. Meas. **31**, 83-87 (1982).
5. W. H. Oskay, S. A. Diddams, E. A. Donley, T. M. Fortier, T. P. Heavner, L. Hollberg, W. M. Itano, S. R. Jefferts, M. J. Delaney, K. Kim, F. Levi, T. E. Parker, J. C. Bergquist, "Single-atom optical clock with high accuracy," Phys. Rev. Lett. **97**, 020801, 1-4 (2006).
6. C. W. Oates, E. A. Curtis, L. Hollberg, "Improved short-term stability of optical frequency standards: approaching 1 Hz in 1 s with the Ca standard at 657 nm," Opt. Lett. **25**, 1603-1605 (2000).
7. L. S. Ma, Z. Bi, A. Bartels, K. Kim, L. Robertsson, M. Zucco, R. S. Windeler, G. Wilpers, C. Oates, L. Hollberg, S. A. Diddams, "Frequency uncertainty for optically referenced femtosecond laser frequency combs," IEEE J. Quantum Electron. **43**, 139-146 (2007).
8. A. Bartels, C. W. Oates, L. Hollberg, S. A. Diddams, "Stabilization of femtosecond laser frequency combs with subhertz residual linewidths," Opt. Lett. **29**, 1081-1083 (2004).
9. I. Coddington, W. C. Swann, L. Lorini, J. C. Bergquist, Y. Le Coq, C. W. Oates, Q. Quraishi, K. S. Feder, J. W. Nicholson, P. S. Westbrook, S. A. Diddams, and N. R. Newbury, "Coherent optical link over hundreds of metres and hundreds of terahertz with subfemtosecond timing jitter," Nat. Photonics **1**, 283-287 (2007).

10. N. R. Newbury, W. C. Swann, I. Coddington, L. Lorini, J. C. Bergquist, S. A. Diddams, "Fiber laser-based frequency combs with high relative frequency stability," in *Proc. 2007 Joint Mtg. IEEE Intl. Freq. Cont. Symp. and EFTF Conf.*, Geneva, Switzerland, pp. 980-983, (2007).
11. W. C. Swann, J. J. McFerran, I. Coddington, N. R. Newbury, I. Hartl, M. E. Fermann, P. S. Westbrook, J. W. Nicholson, K. S. Feder, C. Langrock, M. M. Fejer, "Fiber-laser frequency combs with subhertz relative linewidths," Opt. Lett. **31**, 3046-3048 (2006).
12. A. Bartels, R. Gebs, M. S. Kirchner, S. A. Diddams, "Spectrally resolved optical frequency combs from a self-referenced 5 GHz femtosecond laser," Opt. Lett. **32**, 2553-2555 (2007).
13. T. Wilken, T. W. Hänsch, R. Holzwarth, P. Adel, M. Mei, "Low Phase Noise 250 MHz Repetition Rate Fiber fs Laser for Frequency Comb Applications," Conference on Lasers and Electro-Optics (CLEO), CMR3 , Baltimore, Maryland , USA, 6-11 May, (2007).
14. A. Bartels, "Gigahertz femtosecond lasers," in *Femtosecond optical frequency comb technology Principle, operation and application,* J. Ye, S. T. Cundiff, eds. (Springer, New York, 2005), pp. 78-96.
15. J. J. McFerran, L. Nenadović, W. C. Swann, J. B. Schlager and N. R. Newbury, "A passively mode-locked fiber laser at 1.54 μm with a fundamental repetition frequency reaching 2 GHz," Opt. Express **15**, 13155-13166 (2007).
16. C. G. Leburn, A. A. Lagatsky, C. T. A. Brown, W. Sibbett, "Femtosecond Cr^{4+}:YAG laser with 4 GHz pulse repetition rate," Electronics Letters **40**, 805-807 (2004).
17. X. P. Zhang, J. Hebling, A. Bartels, D. Nau, J. Kuhl, W. W. Rühle, H. Giessen, "1-GHz-repetition-rate femtosecond optical parametric oscillator," Appl. Phys. Lett. **80**, 1873-1875 (2002).
18. J. Jiang, T. Hasama, "Harmonic repetition-rate femtosecond optical parametric oscillator," Appl. Phys. B **74**, 313-317 (2002).
19. D. S. Butterworth, S. Girard, D. C. Hanna, "A simple technique to achieve cavity-length stabilisation in a synchronously pumped optical parametric oscillator," Opt. Commun. **123**, 577-582 (1996).
20. E. S. Wachman, D. C. Edelstein, C. L. Tang, "Continuous-wave mode-locked and dispersion-compensated femtosecond optical parametric oscillator," Opt. Lett. **15**, 136-138 (1990).
21. Y. Kobayashi, K. Torizuka, "Carrier-phase control among subharmonic pulses in a femtosecond optical parametric oscillator," Opt. Lett. **26**, 1295-1297 (2001).
22. A. Bartels, T. Dekorsy, H. Kurz, "Femtosecond Ti:sapphire ring laser with a 2-GHz repetition rate and its application in time-resolved spectroscopy," Opt. Lett. **24**, 996-998 (1999).
23. M. E. Klein, A. Robertson, M. A. Tremont, R. Wallenstein, K.-J. Boller, "Rapid infrared wavelength access with a picosecond PPLN OPO synchronously pumped by a mode-locked diode laser," Appl. Phys. B **73**, 1-10 (2001).
24. J. Sun, B. J. S. Gale, D. T. Reid, "Testing the parametric energy conservation law in a femtosecond optical parametric oscillator," Opt. Express **15**, 4378-4384 (2007).
25. M. Zimmermann, C. Gohle, R. Holzwarth, Th. Udem, T. W. Hänsch "Optical clockwork with an offset-free difference-frequency comb: accuracy of sum- and difference-frequency generation," Opt. Lett. **29**, 310-312 (2004).

1. Introduction

Visible continuous-wave (cw) lasers with subhertz linewidths locked to a narrow clock transition of a single trapped ion or an ensemble of laser-cooled neutral atoms produce a stable optical frequency [1], [2], [3], whose instability may ultimately reach the 10^{-18} level [4]. Recently, such optical frequency standards have been reported with a fractional frequency uncertainty below 7×10^{-17} and an instability of 4×10^{-15} at 1 s gate time [5], [6]. Femtosecond laser frequency combs (FLFC) are a convenient means for transferring the properties of such optical frequency standards to other optical frequencies and to the microwave domain. FLFCs based on mode-locked Ti:sapphire lasers have so far shown the best performance for optical and microwave frequency synthesis relative to optical frequency standards in terms of uncertainty (8×10^{-20}), instability (1.8×10^{-17} at 1 s gate time) [7] and residual linewidth (23 mHz) [8]. They are, however, not capable of reaching wavelengths beyond approximately 1200 nm, thus far precluding their use for frequency dissemination over long-distance fiber networks at telecom wavelengths. Thus currently, the 1550 nm region is mostly accessed with Erbium-doped femtosecond (fs) fiber lasers. A relative uncertainty of 5.3×10^{-19} [9], an instability of 6×10^{-17} at 1 s gate time [10] and a residual linewidth of 300 mHz [11] has been reported for these sources. While this performance begins to approach that of the best Ti:sapphire systems, a unique advantage of the latter is the fact that they reach repetition rates as high as 5 GHz [12].

The highest repetition rate for a self-referenced Er fiber system is 250 MHz [13]. High repetition rates are beneficial because of a greater power per mode and the corresponding higher signal-to-noise ratio for beat signals versus cw lasers [14]. While 1550 nm mode-locked lasers at GHz repetition rates have recently become available based on Yb-Er fibers and Cr^{4+}:YAG crystals, self-referencing of such sources has not yet been demonstrated, likely due to their limited peak intensity [15], [16].

Here, we pursue an alternative approach that aims at taking advantage of the unique performance of Ti:sapphire based systems by transferring their properties to the 1550 nm region using a nonlinear conversion step. To this end, we have constructed a compact femtosecond OPO operating at 1558 nm, that is synchronously pumped by a powerful Ti:sapphire femtosecond laser with 1 GHz repetition rate. While 1 GHz femtosecond OPOs have been demonstrated before at 1300 nm using pumping concepts with several pulses in the cavity [17], [18], this is the first demonstration of fundamental pumping at 1 GHz repetition rate with a single pulse in the cavity. A significant advantage of fundamental pumping is the fact that nonlinear gain is supplied upon each passage through the OPO crystal. While previous stabilization schemes for femtosecond OPOs stabilize the spectral envelope [19], [20], we introduce a method where both the spectral envelope and the underlying frequency comb of the signal and idler output are stabilized relative to each other and are absolutely stabilized if the pump laser comb is fixed. Our concept is similar to the work of Kobayashi and Torizuka performed with a femtosecond OPO at 1275 nm, where different sum frequency generation products of the pump laser and the OPO were stabilized relative to each other in order to produce phase-locked subharmonic optical pulses [21]. Our scheme recycles a large fraction of the 800 nm pump power, which could be used for producing broadband spectra covering the $500 - 1000$ nm region in a nonlinear fiber. Thus, our concept may be specifically useful for bridging the gap between the visible frequencies of many local oscillators of current optical frequency standards and linking them to the 1550 nm region. In addition to possible use as an FLFC, we envision applications of this system in other spectroscopic areas such as two-color optical pump-probe experiments.

2. Optical setup and performance

Figure 1 shows the experimental setup. The Ti:sapphire based femtosecond ring laser [22] is pumped by 6.5 W of 532 nm cw light. It emits 30 fs pulses at a center wavelength of 800 nm with a repetition rate of 1 GHz and provides 1.2 W of average output power. The output pulse train is coupled into the OPO ring cavity through its output coupler OC2 (97 % transmission for $740 - 950$ nm, 2 % transmission from 1430 nm to 1650 nm) and focused into a periodically poled lithium niobate (PPLN) crystal by means of the curved mirror M1. The OPO cavity is completed by the curved mirror M2 and the flat mirror M3. M1, M2 and M3 are high reflective for 750 to 850 nm and 1400 to 1625 nm. Both curved mirrors M1 and M2 have 30 mm radius of curvature, the same value as is used in the Ti:sapphire pump laser. In contrast to typical pump-coupling schemes for OPOs [17], [18] additional pulse broadening due to a focusing lens is avoided with the present setup. At the same time, the distance travelled by the pump pulses from the Ti:sapphire crystal to the PPLN crystal approximately matches the cavity length of the pump laser and the OPO, thus ensuring that the pump pulses are focused at the center between M1 and M2, where the PPLN crystal is located. A residual mode-mismatch between the pump- and the signal beam in the PPLN crystal, due to the differing wavelengths, may be eliminated by adjusting the M1-M2 distance. The latter provides leverage on the signal beam waist when the OPO cavity is operated close to the inner edge of its stability range. The setup is particularly useful for frequency comb applications, because approximately 900 mW of residual pump light exit through OC2 and can be recycled in order to produce an octave spanning spectrum and measure the pump laser carrier-envelope offset frequency $f_{0,p}$. The 1 mm long multigrating
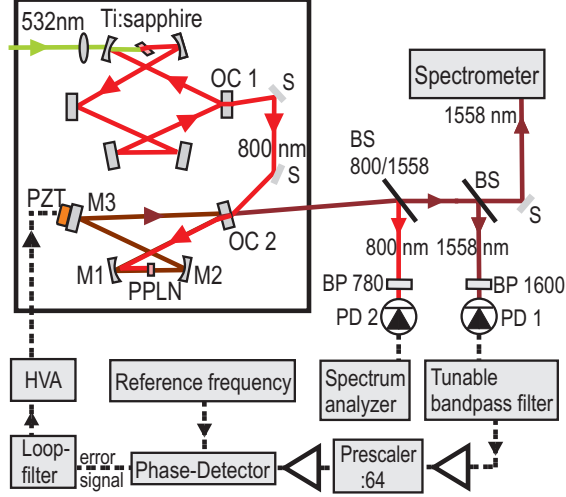
Fig. 1. Experimental setup of the Ti:sapphire based femtosecond pump laser, the OPO cavity and the stabilization electronics. Both the Ti:sapphire and the OPO cavity are enclosed in one common box (31 cm×36 cm×9 cm) to reduce environmental perturbations. Solid lines correspond to optical paths and dashed lines to electrical paths. OC1, OC2: output coupler of the Ti:sapphire and the OPO cavity, PPLN: multigrating periodically poled lithium niobate, PZT: piezoelectric transducer, M1, M2, M3: OPO cavity mirrors, PD1, PD2: photodiodes, BS: beamsplitter, BP: optical bandpass filter, S: silver mirror (not part of the cavities), HVA: high voltage amplifier.

PPLN crystal is antireflection coated for wavelengths between 750 and 850 nm and between 1500 and 1750 nm. The quasi-phase matching (QPM) period Λ can be varied from 19.5 to 21.3 μm in 0.2 μm steps. Here we used $\Lambda = 19.9\,\mu$m. The PPLN crystal is heated to 165 °C in order to avoid photorefractive damage. For fundamental synchronous pumping the signal pulse round-trip time in the OPO cavity has to be matched to the 1 GHz pump laser repetition rate. To achieve this, the OPO ring cavity length is roughly preset to 30 cm. More precise cavity length control is enabled by using a translation stage to adjust the OC2 position and a piezoelectric transducer (PZT) supporting M3. Here, cavity length tuning [23] of the signal center wavelength is continuously feasible from 1480 to 1580 nm. The signal output power for a center wavelength at 1558 nm is 80 mW and its spectral full width at half maximum (FWHM) is 40 nm. This bandwidth supports 65 fs pulses. The OPO pump-signal conversion efficiency is approximately 8 % and the pump threshold for OPO oscillation is 710 mW. The bulk of the idler light is not resonant in the cavity and is transmitted through the cavity mirrors.

3. Stabilization scheme

The individual teeth of the pump- f_p, signal- f_s and idler-frequency combs f_i are expressed as

$$
\begin{aligned}
f_p &= k_p \times f_{rep} + f_{0,p} \\
f_s &= k_s \times f_{rep} + f_{0,s} \\
f_i &= k_i \times f_{rep} + f_{0,i} \quad,
\end{aligned}
\tag{1}
$$

where $k_{p,s,i}$ are integers enumerating the comb teeth, f_{rep} and $f_{0,p,s,i}$ are the repetition rates and the carrier envelope offset frequencies of the pump-, signal- and idler-frequency combs. k_s is on the order of 2×10^5. The signal- and idler pulse trains have the same repetition rate f_{rep} as the

pump. The comb offset frequencies $f_{0,p,s,i}$ are related to each other through energy conservation

$$f_{0,p} = f_{0,s} + f_{0,i} \quad . \tag{2}$$

To support synchronous pumping, the signal light group-delay in the OPO cavity must at all times equal the inverse pump laser repetition rate. In order to fulfill this condition, changes of the OPO cavity length relative to the pump laser cavity length, e.g. through external perturbations, automatically cause a shift in the signal light spectral envelope λ_s mediated by group-delay dispersion:

$$\frac{d\lambda_s}{d\Delta L} = -\frac{1}{L_C} \times \left(\frac{dn_g}{d\lambda_s}\right)^{-1} . \tag{3}$$

Here, ΔL is the offset between the geometrical cavity lengths of the OPO and the pump laser, L_C is the length of the PPLN crystal and n_g the group index of the signal pulse in the PPLN. This effect is widely used for wavelength tuning of synchronously pumped OPOs [23]. As a second condition, the signal comb teeth resonating in the OPO cavity must fulfill the standing wave condition. For an arbitrary resonant signal comb tooth this is written as

$$f_s(L) = \frac{p \times \bar{c}}{L} = k_s \times f_{rep} + f_{0,s} \quad , \tag{4}$$

where $\bar{c}$ is the mean phase velocity in the cavity and p the integer number of standing signal waves fitting into the OPO cavity. The consequence of Eqs. (3) and (4) is that a change in the OPO cavity length L changes the phase-delay but not the group delay for the signal light. Thus, $f_{0,s}$ can be varied independent of f_{rep} via L. The envelope and underlying frequency comb of the non-resonant idler output follow the signal output according to energy conservation. In the
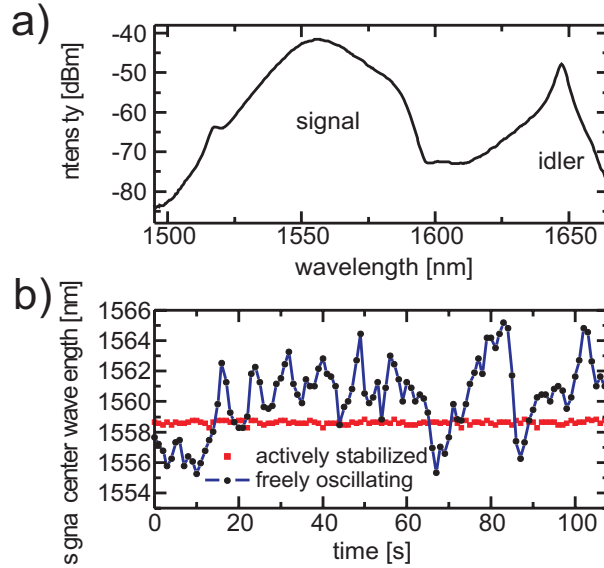

Fig. 2. a) Signal and idler spectra of the actively stabilized OPO. Note the spectral overlap at 1600 nm. As the OPO mirrors are not high reflective for wavelengths larger than 1625 nm, the non-resonant part of the idler spectrum is suppressed. The quasi-phase matching period was $\Lambda = 19.9\,\mu$m.
b) Signal center wavelength versus time for the actively stabilized and freely running OPO. The spectrometer resolution is 0.3 nm.

present experiment the OPO is operated in a nearly degenerate regime, where the signal and idler spectra exhibit a partial overlap around 1600 nm (Fig. 2(a)). By detecting light in this
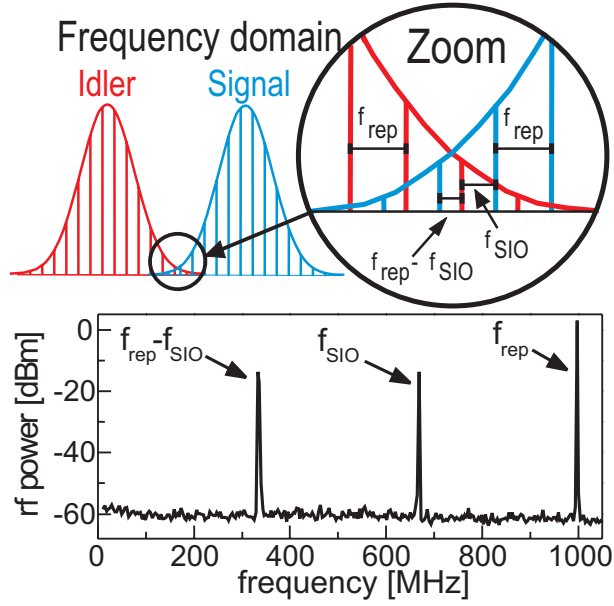

Fig. 3. Top: Illustration of the origin of the radio frequency (RF) beats.
Bottom: A typical RF measurement showing the corresponding beats.

overlap region with photodiode PD1 (InGaAs p-i-n diode) a signal with a radio frequency (RF) spectrum as shown at the bottom of Fig. 3 is detected. The contribution at 1 GHz represents the repetition rate f_{rep}. The peaks labelled f_{SIO} and $f_{rep} - f_{SIO}$ are beats between the signal- and idler frequency combs (see illustration at the top of Fig. 3) that are only detectable in the overlap region of the signal- and idler spectra at around 1600 nm. The beat at f_{SIO} represents the offset between the signal- and idler frequency combs (SIO) and is defined as

$$f_{SIO} := f_{0,i} - f_{0,s}. \tag{5}$$

Under the assumption that the repetition rate f_{rep} and the carrier-envelope offset frequency $f_{0,p}$ of the pump laser are constant, an active stabilization of f_{SIO} via the OPO cavity length L (Eq. (4)) fixes $f_{0,s}$ and $f_{0,i}$ through energy conservation (Eq. (2)) and thus the positions of the signal- and idler frequency combs relative to each other (illustration Fig. 3) and to the pump frequency comb. However, in the present experimental setup (Fig. 1) neither $f_{0,p}$ nor f_{rep} have been actively stabilized and are thus drifting within a typical range of approximately 100 kHz and 100 Hz, respectively. Yet, with f_{SIO} actively stabilized via L, the resulting residual fluctuations on $f_{0,s}$ and $f_{0,i}$ are negligible compared to $k_s \times f_{rep}$ (approximately 10^{-9}). Thus the feedback on f_{SIO} forces the OPO cavity length L to follow f_{rep} and thus the pump laser cavity length with a residual relative error of approximately 10^{-9}. This in turn leads to a well-stabilized signal center wavelength λ_s through Eq. (3).

A schematic of the active feedback loop used for signal frequency comb stabilization is shown in Fig. 1. The OPO output is separated from the Ti:sapphire pump light using a dichroic beamsplitter (BS 800/1558), reflecting wavelengths between 750 and 850 nm and transmitting light between 1500 and 1650 nm. Afterwards the degenerate part of the OPO spectrum is isolated

from the rest using an optical bandpass filter at 1600 nm with a transmission bandwidth of 10 nm (BP 1600). After this bandpass filter approximately $10\,\mu$W of optical power were present. For the feedback loop, f_{SIO} is isolated with a tunable RF bandpass filter ($500 - 1000$ MHz). For an increased operating range f_{SIO} is divided by 64 using a prescaler. The subsequent digital phase detector compares $f_{SIO}/64$ with a reference frequency, obtained from a signal generator and provides an error signal. This error signal is supplied to the PZT via an adjustable loop filter and a high voltage amplifier (HVA) such that $f_{SIO}/64$ is stabilized to the reference frequency.

4. Characterization of the stabilization

In Fig. 2(b) the signal center wavelength is shown over a period of 110 seconds for the actively stabilized and the freely oscillating OPO. In the freely running case the instability amounts to 4.3 nm, mostly caused by environmental perturbations to the OPO- and pump laser cavity length. These fluctuations are suppressed to better than 0.15 nm when the feedback loop is engaged (limited by the 0.3 nm resolution of the spectrometer). In the PPLN crystal the second harmonic (SH) of the signal frequency comb is also generated. Its spectrum partially overlaps with the Ti:sapphire pump spectrum at around 780 nm. Using energy conservation (Eq. (2)) and the definition of f_{SIO}, the offset f_{2SPO} between the frequency-doubled signal comb $2 \times f_{0,s}$ and the pump comb $f_{0,p}$, that can be detected at 780 nm, is expected to be

$$f_{2SPO} := f_{0,p} - 2 \times f_{0,s} = f_{0,s} + f_{0,i} - 2 \times f_{0,s} = f_{SIO}. \tag{6}$$

Thus, a beat signal detected with PD2 (Si p-i-n diode) at 780 nm can be used for an out-of-loop characterization of the signal frequency comb stabilization at 1600 nm. For a first characteriza-
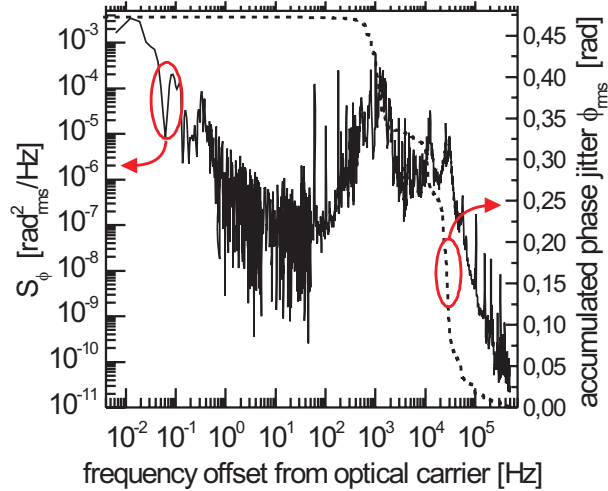

Fig. 4. Out-of-loop measurement of the power spectral density of phase fluctuations S_Φ for the beat at the frequency f_{SIO} actively stabilized at 748.8 MHz. The corresponding numerically calculated accumulated phase jitter Φ_{RMS} is plotted versus the axis on the right hand side.

tion of the signal frequency comb stabilization, the beat at the frequency f_{SIO} was phase-locked to an external reference at 748.8 MHz. Using a vector signal analyzer, the power spectral density (PSD) of phase fluctuations $S_\Phi(f)$ of the beat frequencies detected at 1600 nm (in-loop signal) and at 780 nm (out-of-loop signal) have been measured (see Fig. 4 for out-of-loop PSD

spectrum). From these phase noise data the root-mean-square (RMS) accumulated phase jitter

$$\Phi_{RMS}(f_{min}, f_{max}) := \left(\int_{f_{min}}^{f_{max}} S_\Phi(f) \, df \right)^{1/2} \tag{7}$$

was numerically calculated (see plot vs. right axes in Fig. 4). For the integration limits $f_{min} = 6.25\,\text{mHz}$ and $f_{max} = 0.5\,\text{MHz}$ the calculation results in $\Phi_{RMS} = 0.461\,\text{rad}$ for the in-loop RF-signal and $\Phi_{RMS} = 0.472\,\text{rad}$ for the out-of-loop RF-signal. From these values we infer that the linewidth of the signal frequency comb relative to the pump frequency comb can be at the level of a few millihertz. For the Ti:sapphire pump laser FLFC, a residual linewidth of 23 mHz has been demonstrated earlier, when locked to an optical reference [8]. Thus, if the entire system were actively stabilized to an optical frequency standard it would be capable of transferring the coherence of the optical standard to the 1550 nm region with a linewidth limited only by the performance of the Ti:sapphire system.

For a second characterization of the stabilized signal frequency comb the beat at the frequency f_{SIO} was continuously phase-locked to 631 MHz for 1650 s. At the same time a simultaneous frequency counting of f_{SIO} was performed (in-loop characterization) and of f_{2SPO} (out-of-loop characterization) using two frequency counters (1 s gate time, 12-digit/s resolution). Both frequency counters were referenced to the same low-noise reference (H-maser). From the series of counter readings, we calculate the Allan deviation σ_y normalized to the optical frequency 193.55 THz at which the f_{SIO}-beat is detected to obtain a measure of the signal comb's residual frequency instability. For the in-loop measurement σ_y amounts to 1.36×10^{-17}, the out-of-loop value amounts to 1.46×10^{-17} at 1 s gate time. This performance implies that the nonlinear conversion step using the OPO does not compromise the performance of the best stability yet demonstrated for the Ti:sapphire pump laser. Under the assumption that parametric downconversion and SHG are independent processes, the frequency counting experiment also permits a test of energy conservation during these processes. While we are not aware of a theory explicitly predicting a violation of Eq. (2), processes like Raman or Brillouin scattering might in principle lead to energy depositions in the nonlinear crystal. If there were such a violation, this would cause an offset between the in-loop and the out-of-loop counter data. From an analysis of the mean values, we observe no such effect within an uncertainty of $1.22 \times 10^{-4}\,\text{Hz}$. This reduces the possible error in Eq. (2) by a factor 10^9 compared to similar experiments where the precision of parametric downconversion in a femtosecond OPO was verified to be better than 200 kHz [24]. We thus conclude that energy is conserved in the combined parametric downconversion and subsequent SHG process with a fractional uncertainty of 6×10^{-19}. Similar to previous tests of energy conservation during single-pass difference frequency generation and sum-frequency generation [25], this interpretation does not include the possibility that there may be correlated errors in both processes that cancel exactly.

Finally it is mentioned, that it is also possible to actively stabilize the signal frequency comb by means of the beat frequency f_{2SPO} detected at 780 nm and using the beat frequency f_{SIO} detected at 1600 nm for the out-of-loop characterization.

5. Conclusion and outlook

In conclusion we have demonstrated a 1 GHz repetition rate, partially degenerate femtosecond OPO generating a signal frequency comb centred at 1558 nm with a spectral full width at half maximum of 40 nm. In the partially overlapping region of the signal- and idler spectra at around 1600 nm a beat at the radio frequency f_{SIO} was detected, which represents the offset of the signal-idler frequency combs. Phase-locking f_{SIO} to an external reference stabilizes the signal- and idler frequency combs relative to each other (at 1 s gate time, out-of-loop Allan deviation $\sigma_y = 1.46 \times 10^{-17}$, accumulated phase jitter $\Phi_{RMS} = 0.472$ rad) as well as the center

wavelengths of their spectral envelopes (instability of ± 0.15 nm, spectrometer resolution limited). Following this approach for a Ti:sapphire femtosecond laser frequency comb where the repetition rate f_{rep} and the comb offset frequency $f_{0,p}$ are stabilized to an optical frequency standard, it seems feasible to transfer the unique properties (uncertainty 8×10^{-20}, instability 1.8×10^{-17} in 1 s [7], 23 mHz optical linewidth [8]) of GHz repetition rate femtosecond Ti:sapphire lasers into the 1550 nm region. Among other things, this would potentially be useful for precision frequency dissemination over long-distance fiber networks.